

Unimolecular Micelles of Amphiphilic Cyclodextrin-Core Star-Like Copolymers with Covalent pH-Responsive Linkage of Anticancer Prodrugs

Jia, Tao; Huang, Shuo; Yang, Cangjie; Wang, Mingfeng

2016

Jia, T., Huang, S., Yang, C., & Wang, M. (2017). Unimolecular Micelles of Amphiphilic Cyclodextrin-Core Star-Like Copolymers with Covalent pH-Responsive Linkage of Anticancer Prodrugs. *Molecular Pharmaceutics*, 14(8), 2529-2537.

<https://hdl.handle.net/10356/85476>

<https://doi.org/10.1021/acs.molpharmaceut.6b00708>

© 2016 American Chemical Society. This is the author created version of a work that has been peer reviewed and accepted for publication by *Molecular Pharmaceutics*, American Chemical Society. It incorporates referee's comments but changes resulting from the publishing process, such as copyediting, structural formatting, may not be reflected in this document. The published version is available at:
[<http://dx.doi.org/10.1021/acs.molpharmaceut.6b00708>].

Downloaded on 20 Mar 2024 17:56:03 SGT

Unimolecular Micelles of Amphiphilic Cyclodextrin-core Star-like Copolymers with Covalent pH-Responsive Linkage of Anticancer Prodrugs

Tao Jia, Shuo Huang, Cangjie Yang, Mingfeng Wang*

School of Chemical and Biomedical Engineering, Nanyang Technological University,

62 Nanyang Drive, Singapore 637459

ABSTRACT

Multifunctional stable and stimuli-responsive drug delivery systems are important for efficient cancer treatment due to their advantages such as enhanced cancer-targeting efficiency, improved pharmacokinetics, minimized drug leaching and undesirable side effects. Here we report a robust and pH-responsive anticancer drug delivery system based on unimolecular micelles of star-like amphiphilic copolymers. The polymers (denoted as **CPOFs**) were facilely synthesized via one-step atom transfer radical polymerization of functionable benzo-aldehyde and hydrophilic poly[(oligo ethylene glycol) methyl ether methacrylate] as comonomers from the core of heptakis [2,3,6-tri-o-(2-bromo-2-methyl propionyl)]- β -cyclodextrin as the initiator. Doxorubicin (DOX) as an anticancer drug was covalently linked to the benzo-aldehyde groups of **CPOFs** through pH-sensitive Schiff-base bonds. The DOX-conjugated polymers, denoted as **CPOF-DOX**, formed robust unimolecular micelles with an average diameter of 18 nm in aqueous media. More importantly, these unimolecular micelles showed higher drug loading capacity and more controllable drug release characteristics, compared to our previous unimolecular micelles of β -cyclodextrin-poly(lactic acid)-b-poly[(oligo ethylene glycol) methyl ether methacrylates] that physically encapsulated DOX via hydrophobic interaction. Moreover, the **CPOF-DOX** unimolecular micelles could be internalized by human cervical cancer HeLa cells in a stepwise way and showed less cytotoxicity compared to carrier-free DOX. We foresee that **CPOF-DOX** would provide a promising robust

and controllable anticancer drug delivery system for future animal study and clinical trials for cancer treatment.

1. INTRODUCTION

Cancer has remained one of the leading causes of deaths in the world,¹⁻³ despite the fact that intense research in cancer diagnosis and treatment has led to decreased mortality rates in the past years. Among a variety of therapeutic methods for clinical treatment of cancers, chemical therapy remains widely used. For instance, a series of anticancer drugs such as doxorubicin (DOX), camptothecin (CPT), and paclitaxel (PTX) have been developed for cancer therapy.⁴⁻⁶ In order to manipulate the pharmacokinetics of these drugs, reduce the off-target toxicity, and improve the therapeutic efficacy, a myriad of drug delivery systems including liposomes,⁷⁻⁹ polymer-prodrug conjugates,¹⁰⁻¹³ dendrimers,¹⁴⁻¹⁷ inorganic nanoparticles,¹⁸⁻²⁶ and polymer micelles²⁷⁻³⁶ have been developed. In particular, Doxil, which encapsulates anticancer drug DOX in a liposome, was the first nanoparticle drug approved by the U.S. Food & Drug Administration in 1995.³⁷ Genexol-PM, a PTX-loaded micelle from linear poly(ethylene glycol)-*b*-poly(lactic acid) (PEG-*b*-PLA) block copolymers, was approved in Korea in 2007 for breast cancer treatment.^{38,39} In both systems, the drug carrier (either liposome or block copolymer micelle) elongates the drug circulation lifetime in the bloodstream, improves the targeting efficiency towards tumour tissues, and reduces the undesired toxicity to healthy tissues.

Despite the aforementioned exciting advances in cancer treatment, one limitation that still exists in the present liposomal and micellar systems for anticancer drug delivery is their relatively low stability. Both liposomes and conventional block copolymer micelles, which are typically associated with labile hydrophobic interaction, are sensitive to factors such as concentration, pH, and temperature. Such low stability may cause the dissociation of the self-assembling drug carriers and undesired drug leaching and toxicity.

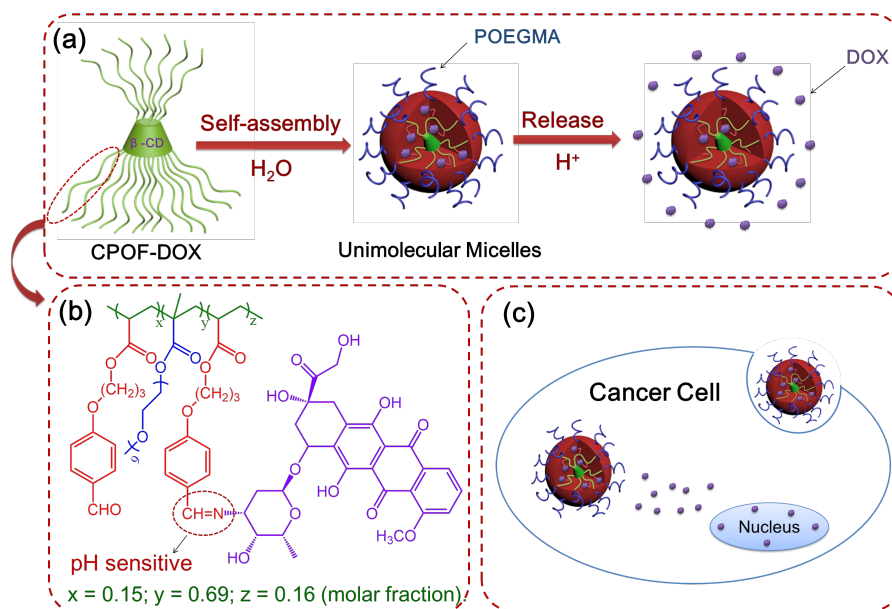
We previously reported a strategy of unimolecular micelles to address the stability problem in conventional block copolymer micelles.³¹ Each unimolecular micelle was formed by an amphiphilic cyclodextrin-core star-like PEG-PLA block copolymer with well-defined chemical structure. These unimolecular micelles could effectively encapsulate anticancer drugs such as DOX in the domain of PLA via hydrophobic interaction and showed more sustainable drug-release behavior compared to carrier-free drug molecules. Despite the robustness of these unimolecular micelles, the relatively weak hydrophobic interaction between the drugs and the polymer matrices may still limit the drug-loading content and lead to potential drug leaching.

Herein, we report a further improved approach by incorporating anticancer prodrugs into the unimolecular micelles via covalent pH-responsive Schiff-base bonds. The experimental design is depicted in Scheme 1. We hypothesized that such covalent linkage with significantly improved stability compared to the noncovalent hydrophobic interaction between anticancer drugs and the micellar carries would increase the drug loading content and further reduce the possibility of drug leaching

during circulation in physiological systems. Furthermore, the pH-sensitive nature of the Schiff-base bonds was expected to further enhance the tumor-targeting release of drugs, given the fact that the tumor microenvironment usually has lower pH compared to normal tissues and blood.⁴⁰ Compared to the previously reported pH-responsive micellar drug carriers associated with labile hydrophobic interaction of linear block copolymers,^{12,27} the enhanced stability of both the unimolecular micelles and the covalent linkage between the polymer carrier and the anticancer drugs in the present system are expected to minimize the premature drug release and the side effect of toxicity.

Specifically, β -cyclodextrin (β -CD) was also utilized as the core to synthesize the star-like amphiphilic copolymers via atom transfer radical polymerization (ATRP). Each arm of the star-like copolymers consists of statistically distributed functionable benzo-aldehyde groups and hydrophilic poly[(oligo ethylene glycol) methyl ether methacrylates] groups (Scheme 1b). Then an anticancer drug DOX was covalently conjugated with the aldehyde groups of the amphiphilic polymer through the primary amine group of DOX by forming a pH-sensitive Schiff-base linkage, which is known to be stable in neutral or alkaline media but readily cleavable under acidic conditions.^{12,13} The chemical structures of the polymers (denoted as **CPOFs**) and the conjugation between the polymers and DOX moieties were characterized by nuclear magnetic resonance (NMR) spectroscopy, Fourier transform infrared (FT-IR) spectroscopy and gel permeation chromatography (GPC). The size, size distribution, stability and in vitro drug release of the unimolecular micelles (denoted as

CPOF-DOXs) at different pH values were analyzed. Finally, the internalization of the unimolecular micelles by HeLa cells and the cytotoxicity versus carrier-free DOX were studied.



Scheme 1. Schematic illustration of the design of β -CD-core star-like copolymer for enhanced intracellular release of anticancer drug (a); chemical structure of each arm in the star-like copolymer (b); internalization of the drug-loading unimolecular micelles by a cancer cell and the following drug release to the nucleus (c).

2. EXPERIMENTAL SECTION

Materials and General Instrumentation. All chemical reagents including 4-hydroxybenzaldehyde, 3-bromopropanol, acryloyl chloride, β -cyclodextrin (β -CD, 99.7%), α -bromoisobutyryl bromide (BIBB, 98%), triethylamine (TEA, 99%), copper (I) bromide (Aldrich, 98.0%), tris [2-(dimethylamino) ethyl] amine (Me_6TREN) and oligo-(ethylene glycol methyl ether methacrylate) (OEGMA, $M_n = 500 \text{ g mol}^{-1}$) were purchased from Sigma-Aldrich (USA) and used as received unless otherwise noted. Copper (I) bromide was purified by washing with acetic acid and methanol three times, respectively, then stored in glove box. OEGMA was passed through a column

of activated basic alumina to remove inhibitors before using. Doxorubicin hydrochloride (DOX•HCl) was obtained from Beijing Hua Feng United Technology CO. Ltd (Beijing, China). All anhydrous solvents including tetrahydrofuran (THF) were also provided by Sigma-Aldrich (USA) and used directly. All the other solvents were analytical grade and provided by the Ctech Global Pte Ltd (Singapore). Dulbecco's Modified Eagle's Medium (DMEM), fetal bovine serum (FBS), penicillin/streptomycin mixture, phosphate buffered saline (PBS), Alexa Fluor® 633 phalloidin, TrypLE™ Express Enzyme (1×), DAPI (4',6-diamidino-2-phenylindole) and PrestoBlue cell viability reagent were purchased from Life Technologies (Singapore). Deionized (DI) water was prepared from Millipore (Bedford, MA, USA). The macroinitiator heptakis [2,3,6-tri-o-(2-bromo-2-methylpropionyl)]-β-cyclodextrin (β-CD-21Br) was synthesized according to literature.⁴¹ The monomer 3-(4-formylphenoxy) propyl acrylate (FPPA) contained functionalized benzaldehyde group was prepared using a two-step synthetic approach. Firstly, 4-(3-hydroxypropoxy) benzaldehyde was formed via simple alkylation of 4-hydroxybenzaldehyde. FPPA was then generated by the esterification reaction. Byproducts from the esterification reaction were removed using column chromatography.

¹H NMR spectra were recorded on a Bruker AV 300 NMR spectrometer (Rheinstetten, Germany) using tetramethylsilane as an internal standard at 25 °C. The size distribution of resulting micelles was determined by dynamic light scattering (DLS) using a BI-200SM (Brookhaven, USA) with angle detection at 90°. The

morphology of the samples was recorded by a TEM Carl Zeiss Libra 120 Plus at an acceleration voltage of 120 kV. Samples for TEM measurements were prepared by the following method: for the micelle samples prepared in water, one droplet of the aliquot was casted on carbon-coated copper grids held by tweezers and dried in air at room temperature. The Fourier transform infrared (FT-IR) spectra were acquired on a Perkin Elmer FT-IR spectrophotometer (USA) using KBr pellets. The number-average molecular weight (M_n) and molecular weight distribution (M_w/M_n) were measured by gel permeation chromatography (GPC) system (Agilent 1260, USA) equipped with waters 1260 pump, a Agilent 1260 refractive index detector, a UV-vis detector and a styragel® HT column. Tetrahydrofuran (THF) was used as the eluent (1 mL min⁻¹), and polystyrene was used as the standard for calibration. Fluorescence spectra were recorded on a Perkin Elmer LS-55 fluorescence spectrometer (Perkin Elmer, USA). Absorption spectra were acquired using a Shimadzu UV-2450 visible spectrophotometer (Shimadzu, Japan). The fluorescence images of cells were acquired using a confocal laser scanning microscopy (LSM 780, Carl Zeiss, Germany).

Synthesis and Characterization. 4-(3-hydroxy-propoxy)-benzaldehyde. To a solution of 4-hydroxybenzaldehyde (6 g, 49.2 mmol) and K₂CO₃ (11.7 g, 83.4 mmol) in DMF (50 mL) was added 3-bromopropanol (5.4 mL, 59.1 mmol). The mixture was stirred at room temperature for 12 h, diluted with H₂O (100 mL), and extracted with EtOAc (3 × 20 mL). The combined organic layers were washed with 1 M NaOH (2 ×), H₂O (1 ×), and brine (1 ×). The organic layer was dried by MgSO₄ and

concentrated to afford 8.2 g (76% yield) of a yellow oil. ^1H NMR (300 MHz, CDCl_3): δ 9.86 (s, 1 H), 7.83 (d, 2 H, $J = 9$ Hz), 7.01 (d, 2 H, $J = 9$ Hz), 4.22 (t, 2 H, $J = 6.3$ Hz), 3.88 (t, 2 H, $J = 9$ Hz), 2.11 (m, 2 H), 1.89 (s, 1 H).

FPPA (3-(4-formylphenoxy) propyl acrylate). A 100 mL round bottom flask was charged with 4-(3-hydroxy-propoxy) -benzaldehyde (5 g, 27.8 mmol), triethylamine (6 mL, 41.8 mmol) and 50 mL of anhydrous THF. The solution contained acryloyl chloride (3.2 mL, 32 mmol) in 6 mL THF was added dropwise to the mixture at 0 $^\circ\text{C}$. The reaction was stirred at room temperature for 12 h after completion of addition. Then the solution was filtered to remove the salt and the crude product was recovered by evaporation of THF. The product was purified by passing through silica column chromatography (eluent: DCM/Hexane = 2/1 v/v). Finally, the product was concentrated and dried in vacuum. Yield: 4.03 g (62%). ^1H NMR (300 MHz, CDCl_3): δ 9.90 (s, 1 H), 7.87 (d, 2 H, $J = 9$ Hz), 7.03 (d, 2 H, $J = 9$ Hz), 6.49 (m, 1 H), 6.19 (m, 1 H), 5.89 (m, 1 H), 4.41 (t, 2 H, $J = 6.3$ Hz), 4.19 (t, 2 H, $J = 9$ Hz), 2.22 (m, 2 H).

CPOF (β -CD-P(OEGMA-FPPA)). Typically, β -CD-21Br (10 mg, 0.05 mmol), CuBr (7.3 mg, 0.05 mmol), and FPPA (840 mg, 3.59 mmol), OEGMA (2.52 g, 5.0 mmol) were dissolved in solvent (3.0 mL THF) in a 10 mL flask, and the solution was degassed with three cycles of freeze-pump-thaw. Then the catalyst Me_6TREN (25.2 μL , 0.05 mmol) was injected into the solution, and the mixture was degassed with two freeze-pump-thaw cycles. The polymerization was carried out at 60 $^\circ\text{C}$ for 24 h. The reaction mixture was diluted with THF and then passed through a short neutral Al_2O_3 column to remove the copper catalyst. The resulting mixture was concentrated and

poured into diethyl ether to precipitate the product. (Yield: 16.2%, $M_{n, GPC} = 49.4$ KDa, $M_w/M_n = 1.78$)

CPOF-DOX (β -CD-P(OEGMA-FPPA-DOX)). DOX·HCl (20 mg) was dissolved in 1 mL of DMSO in the presence of an equivalent of TEA. This solution was added dropwise to a stirred solution of **CPOF** (20 mg, in 1 mL DMSO). The reaction was allowed to proceed at room temperature in the dark. After 12 h, the product was dialyzed against DMSO using a dialysis membrane tube with molecular weight cut-off (MWCO) of 3.5 kDa for 7 days to remove nonreacted DOX. ($M_{n, GPC} = 59.4$ KDa, $M_w/M_n = 1.82$)

Preparation of CPOF unimolecular micelles in different solvents. Typically, **CPOF** unimolecular micelles in DMF were obtained by direct dissolving corresponding copolymer in DMF and stirred for 6 h with a final concentration of 0.5 mg mL⁻¹. The resulting solution was further analyzed by DLS to demonstrate a successful formation of unimolecular micelles. Furthermore, **CPOF** micelles in water were prepared by a dialysis method. Briefly, 1 mL solution of 5.0 mg mL⁻¹ **CPOF** in DMF was added into 10 mL of DI water by pump under sonication with a rate of 1.0 mL min⁻¹, followed by dialysis (MWCO 3500) against deionized water (2 L \times 3) for 72 h to remove organic solvent. The resulting **CPOF** micelles with a concentration of 0.5 mg mL⁻¹ were further analyzed by DLS and TEM.

Preparation of DOX-Polymer (CPOF-DOX) micelles. The purified **CPOF-DOX** dissolved in DMSO was dialyzed against DI water (2 L \times 3) for 72 h to obtain the DOX-polymer micelles. The concentration of resulting **CPOF-DOX** micelles was

adjusted to 2 mg mL⁻¹ for further experiments.

In vitro DOX release. In vitro release profiles of DOX were evaluated by the dialysis method. First, A dialysis bag (MWCO 3500) was filled with 3 mL of **CPOF-DOX** micelles soaked in a tube containing 30 mL of PBS 7.2 or 5.0 in a water bath with gentle shaking at 37 ± 1 °C. At predetermined time intervals, 3 mL of the external buffer was withdrawn and it was replaced with 3 mL of fresh PBS 7.2 or 5.0. Then release concentration of free DOX was calculated based on a calibration curve by fluorescence spectroscopy with an excitation spectrum at 495 nm and emission spectrum at 550 nm. The released total amount of DOX was calculated on the basis of the formula. Above release experiments were tested in triplicate.

$$m_{t-act} = (C_t + \frac{V}{V} \sum_0^{t-1} C_t) V$$

Where m_{t-act} is the actual quantity of DOX·HCl released at time t, C_t is the drug concentration in release fluid at time t measured on fluorescence spectrometer, v is the sampled volume taken at a predetermined time interval, and V is the total volume of release fluid.

Cell culture. HeLa cells were regularly cultured and passaged using DMEM medium supplemented with 10% FBS and 1% penicillin-streptomycin at 37 °C with 5% CO₂ in a humidified incubator.

In vitro cellular uptake by confocal laser scanning microscopy. About 10000 HeLa cells were seeded into a 12-well plate and cultured in 37 °C with 5% CO₂. After 12 h for attachment, free DOX·HCl and **CPOF-DOX** (final DOX concentration: 50 µg mL⁻¹) were added to the medium and incubated with HeLa cells. After

incubation over 2, 12 and 24 h, respectively, the cell culture medium was removed and each well was washed with 1×PBS for five times. After that, cells were fixed by formalin solution for 30 min and then washed by 1×PBS extensively for three times. Then cells were blocked for 30 min in 1×PBS containing 1% (wt/vol) BSA. Then Alexa Fluor® 633 phalloidin diluted 20 times according to the protocol in 1×PBS was added to stain filamentous actin (F-actin) cytoskeleton for 1 h at room temperature. After washing three times, cell nucleus was stained by DAPI for 10 min at room temperature and then the samples were washed three times and then added in fresh 1×PBS. Lasers of 405, 488, and 633 nm were used to excite DAPI, DOX, and Alexa Fluor® 633 phalloidin, respectively. The corresponding fluorescence emissions were recorded by a confocal laser scanning microscopy (LSM 710, Carl Zeiss, Germany) using a band-pass filter combination including 410-507, 493-634, and 638-747 nm for imaging in three individual channels (Objective: EC Plan-Neofluar 20x/0.30 M27; dimension is 1024 ×1024.).

Cytotoxicity. PrestoBlue assay was performed to test the cell viability, in which a nonfluorescent blue compound called resazurin (max.abs = 600 nm) in PrestoBlue® reagent can be reduced by live cells to resorufin (max.abs = 570 nm) which is red in color and highly fluorescent. By measuring the absorbance at 570 and 595 nm, cell viability can be calculated relative to the control cells without drug treatment. The cytotoxicity of **CPOF-DOX** in HeLa cells was studied as below, in which free DOX·HCl was also studied for comparison. Firstly, HeLa cells were seeded into a 96-well plate (5000 cells per well) and cultured at 37 °C with 5% CO₂. After attachment over

night, the culture medium was removed and replaced with fresh medium containing free DOX·HCl and **CPOF-DOX** micelles with varied concentrations for 24, 48 and 72 h, respectively. Then the culture medium was removed and washed by 1×PBS for three times. Then PrestoBlue reagent diluted by DMEM medium was added to each well and incubated at 37 °C with 5% CO₂. At the same time, PrestoBlue reagents diluted by DMEM medium were also added to blank wells without cells as control. After 1 h incubation, the absorbance at 570 nm (reference wavelength is 595 nm) was detected by Plate Reader (Tecan Infinite M200 series Pro, Tecan Asia, Singapore). All samples were tested in five replicates. Cells without treatment were used as control and corresponding cell viability was set as 100%. Data were analyzed according to the protocol. Meanwhile, the cytotoxicity of blank **CPOF** micelles was investigated using HeLa cells through the similar method and protocol.

3. RESULTS AND DISCUSSION

Polymer Synthesis and Characterization. The synthetic route to the target polymer, denoted as β -CD-P(OEGMA-FPPA) (**CPOF**), is shown in Scheme S1 in the Supporting Information. **CPOF** was prepared via ATRP using β -CD-21Br as the macroinitiator, and 3-(4-formylphenoxy) propyl acrylate (FPPA) and OEGMA as the comonomers, resulting in random copolymers with $M_n = 49.4$ kDa, and relatively high M_w/M_n value 1.78. The relatively broad polydispersity may be caused by the relatively high reactivity of the aldehyde groups.⁴²⁻⁴⁷ While only a few examples of aldehyde-containing polymers have been synthesized via reversible addition-fragmentation chain-transfer (RAFT) polymerizations without pre-protecting

the aldehyde-containing monomers,⁴⁸⁻⁵⁰ we noticed that aldehyde groups were often protected before many reactions.⁴²⁻⁴⁵ Although similar aldehyde-protection step may minimize potential side reactions in the synthesis of **CPOF** to obtain the target polymer with a narrower polydispersity and a higher yield, such protection-deprotection procedures can be tedious and could increase the production cost. As a consequence, we used non-protected FPPA directly to synthesize **CPOF** via more facile one-step ATRP, but with some sacrifice of the polymer polydispersity and the yield.

The chemical structure of **CPOF** was characterized with ¹H NMR spectroscopy. The integral ratio of the peak at $\delta = 9.86$ ppm (corresponding to the proton from the aldehyde group) to those at $\delta = 3.35$ and 3.50 ppm (corresponding to ethylene glycol protons of OEGMA) indicates that the molar fraction of the benzo-aldehyde group in polymer **CPOF** is ca. 30%.

CPOF and excess DOX were reacted in DMSO for 12 h in the dark, resulting in formation of Schiff-base bonds between the amine group in DOX and the aldehyde group in the polymer. The free DOX was removed through thorough dialysis against DMSO to obtain the target **CPOF-DOX** conjugate.

The chemical structure of **CPOF-DOX** was characterized by ¹H NMR and FT-IR. The ¹H NMR spectra of **CPOF**, DOX and **CPOF-DOX** are shown in Figure 1. The characteristic peaks of both DOX and **CPOF** can be observed in the DOX-polymer conjugate. In particular, the integral ratio of the signal at 6.5 to 8.0 ppm from aromatic protons to that at 9.86 ppm from the protons of unreacted aldehyde group increases in

CPOF-DOX compared to that in **CPOF**, consistent with linkage of DOX to the polymer. More quantitatively, about 52% of aldehyde groups in **CPOF** were grafted with DOX through the Schiff base linkage. Moreover, the DOX content (DC) in **CPOF-DOX** was 17.0wt% from the NMR analysis, which is consistent with the result ($^{dm}DC = 16.8wt\%$) calculated with a differential mass method according to the equation:

$$^{dm}DC = \frac{m_{total} - m_{unreacted}}{m_{CPOF - DOX}}$$

where m_{total} , $m_{unreacted}$, and $m_{CPOF-DOX}$ are the mass of total DOX, DOX unreacted in reaction mixture and polymer **CPOF-DOX**, respectively. $m_{unreacted}$ is calculated from analysis of the UV-vis absorbance of DOX at 495 nm [Figure S1, Supporting Information]. The drug-loading content of **CPOF-DOX** here is obviously higher than that ($\leq 10wt\%$) in our previously reported star-like **β -CD-PLA-*b*-POEGMA** block copolymer micelles in which DOX was encapsulated via hydrophobic interaction. We believe that such higher drug-loading content in **CPOF-DOX** is mainly contributed by the improved stability of Schiff-base linkage between **CPOF** and DOX in comparison to the relatively weak hydrophobic interaction between **β -CD-PLA-*b*-POEGMA** and DOX.

The FT-IR spectrum (Figure S2, Supporting Information) of **CPOF-DOX** and **CPOF** clearly shows the attenuation of the signal at 1720 cm^{-1} from the C=O in the aldehyde groups and the appearance of a new vibrational band at 1650 cm^{-1} from C=N in the Schiff base linkage, which further proves the conjugation of DOX to the polymers.

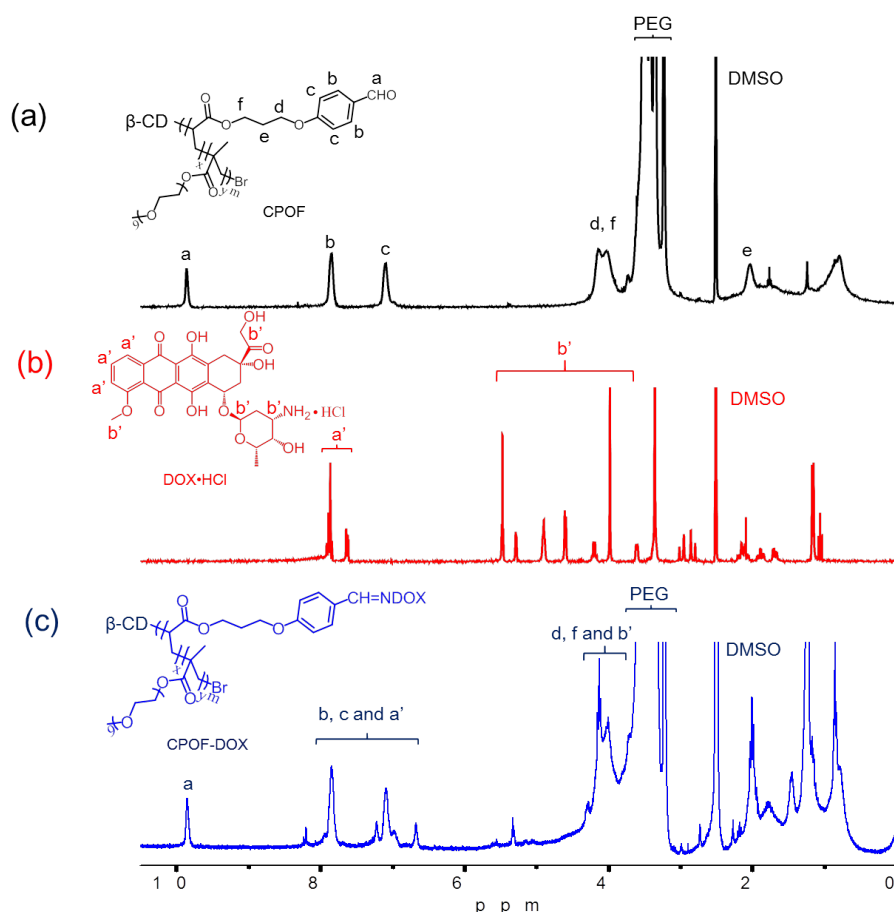


Figure 1. The chemical structure and ^1H NMR spectra of CPOF (a), DOX·HCl (b) and CPOF-DOX (c).

The successful conjugation of DOX to **CPOF** was also verified by GPC measurement (Figure 2). While the precursor **CPOF** showed a monomodal peak at 6-8 min from the refractive index (RI) detector and no signal from the UV-vis detector at 500 nm, DOX·HCl was sensitive to the UV-vis detector (broad peak at 10 min in Figure 2b) but no detectable signals from the RI detector.¹³ After the conjugation reaction, the chromatogram of the resulting **CPOF-DOX** before purification via dialysis showed two peaks from the UV-vis detector, one at 6-8 min (elution time) corresponding to DOX attached to **CPOF**, and the other at 9-13 min corresponding to nonreacted DOX. After thorough purification via dialysis against

DMSO, a monomodal peak at 6-8 min was detected by both RI and UV-vis detectors, whereas the peak from the excess free DOX at 9-13 min completely disappeared in the UV-vis trace. These results further provide strong evidence for the covalent linkage of DOX to **CPOF** polymers as well as the purity of the products.

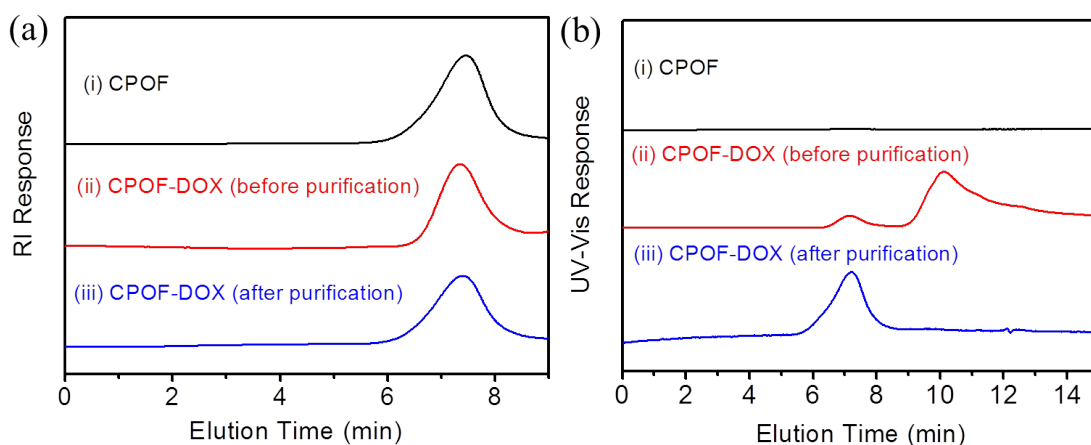


Figure 2. The GPC traces of CPOF and CPOF-DOX (a: RI traces; b: UV-vis traces, wavelength: 500 nm)

Characterization of Unimolecular Micelles. The star-like copolymers, both **CPOF** and **CPOF-DOX**, are easily soluble in water without any external assistance. The size and size distribution of **CPOF** in water as well as in DMF as control (Figure S3 and Table S1, Supporting Information) were measured with dynamic light scattering (DLS). We first studied the concentration-dependence (50, 100 and 500 $\mu\text{g mL}^{-1}$) to examine the possibility of intermolecular aggregation. Similar to our previously reported $\beta\text{-CD-PLA-}b\text{-POEGMA}$ block copolymers,³¹ there was little change of the average hydrodynamic diameter (16 nm) when the concentration of the aqueous solution of **CPOF** was decreased from 500 to 50 $\mu\text{g mL}^{-1}$, which suggests the formation of unimolecular micelles. These results imply that the statistical distribution of FPPA and OEGMA with a molar ratio of 3:7 in each arm of the $\beta\text{-CD-core}$

star-like copolymers (**CPOF**) has no obvious effect on the colloidal stability of unimolecular micelles. In addition, the DLS measurement of CPOF in DMF at 500 $\mu\text{g mL}^{-1}$ gave an average hydrodynamic diameter of 24 nm, which is slightly larger than that (16 nm) of the same polymer at the same concentration in water. Such size difference could be rationalized by the fact that **CPOF** is significantly stretched in DMF as a common good solvent for both PFPPA and POEGMA segments, whereas the PFPPA segments in **CPOF** are collapsed in water which is a selective good solvent for POEGMA. These results suggest that there was no obvious intermolecular aggregation for **CPOF** at the tested concentrations (50 to 500 $\mu\text{g mL}^{-1}$) in water and confirm the formation of unimolecular micelles under the present experimental conditions. Moreover, it appears that an amphiphilic block copolymer structure in each arm of the β -CD-core star-like copolymers is not necessary to form colloidally stable unimolecular micelles, which may simplify the polymer synthesis and reduce the synthetic cost in future scaling-up.

The sizes and morphologies of **CPOF** unimolecular micelles in water before and after loading with DOX were further characterized with transmission electron microscopy (TEM). The results shown in Figure 3 indicate that most of the unimolecular micelles appeared spherical, but with a larger size distribution than those micelles formed by **β -CD-PLA-*b*-POEGMA** block copolymers³¹ which had a narrower polydispersity index than **CPOF**. The average diameter of the **CPOF-DOX** micelles measured from the TEM images was 8.9 ± 2.6 nm, which was slightly larger than that (8.1 ± 3.1 nm) of the blank **CPOF** micelles. The average size of the

micelles measured in dry state here by TEM was about 10 nm smaller than that measured by DLS in hydrated state in water.

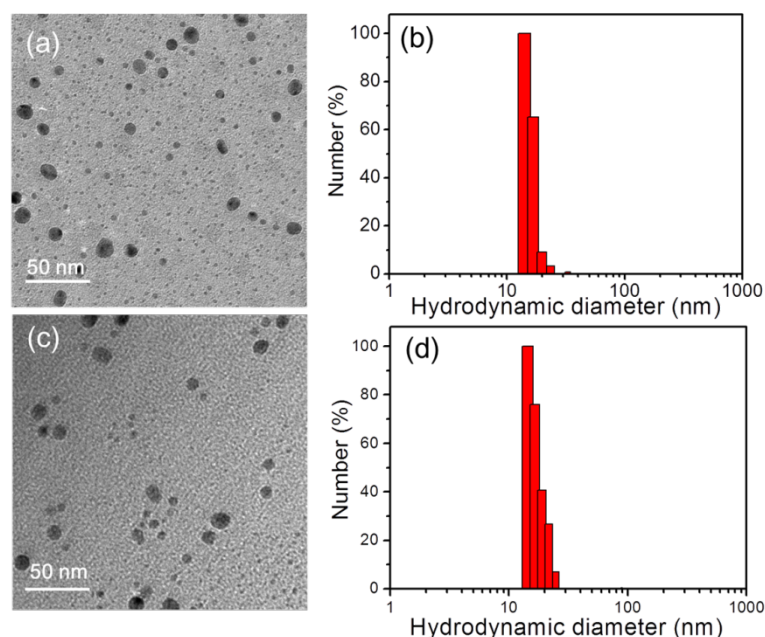


Figure 3. Representative TEM images (a, c) and DLS histograms (b, d) of unimolecular micelles from water (a, b: CPOF ($50 \mu\text{g mL}^{-1}$ in water); c, d: CPOF-DOX ($50 \mu\text{g mL}^{-1}$ in water)). The average hydrodynamic diameter measured by DLS is 15.7 nm for CPOF and 17.8 nm for CPOF-DOX micelles. (The fraction of the largest population of the micelles was normalized as 100% in the y axes of the DLS histograms (b, d))

The UV-vis spectrum (Figure S4, Supporting Information) of **CPOF-DOX** shows significantly enhanced absorption around 500 nm that is attributed to the incorporated DOX. The red shift of the maximum absorption of **CPOF-DOX** compared to that of the pristine DOX·HCl in water or in DMSO is presumably attributed to intermolecular aggregation of DOX in the unimolecular micelles. This phenomenon is in contrast to

the blue shift of DOX physically encapsulated into the hydrophobic core of our previously reported star-like **β -CD-PLA-*b*-POEGMA** block copolymer micelles,³¹ presumably due to the relatively low drug content as well as good miscibility of DOX in the PLA matrices.

To further prove the intermolecular aggregation of DOX in **CPOF-DOX**, we characterized the UV-vis absorption and particle sizes of two control samples: neutralized DOX in DMSO and **CPOF-DOX** in DMSO. The results (Figures S4-6, Supporting Information) show that both the maximal absorption and the onset of neutralized DOX in DMSO are significantly red-shifted, compared to the absorption of DOX•HCl in water or DMSO. In contrast, the absorption spectrum of **CPOF-DOX** in DMSO is comparable to that of the same polymer in water, and both show less red shift compared to that of DOX•HCl in water. DLS measurement (Figure S6 and Table S2, Supporting Information) was conducted further to detect the aggregation of DOX in DMSO (DOX•HCl in DMSO as control). DOX•HCl was completely dissolved in DMSO, without any aggregation at the following three different concentrations: 6.25, 9.0, and 12.5 $\mu\text{g mL}^{-1}$. In contrast, the neutralized DOX showed obvious intermolecular aggregation in DMSO, resulting in increasing particle sizes from 10 nm to 10 μm with the increase of the concentration from 6.25 to 12.5 $\mu\text{g mL}^{-1}$. These results, consistent with red-shift and broadening of the absorption spectra, suggest some extent of intermolecular aggregation of the DOX units in **CPOF-DOX** unimolecular micelles.

In Vitro Drug Release Study. Figure 4 shows the *in vitro* drug release profiles of

CPOF-DOX micelles under physiologically simulated conditions (pH 7.2) compared to slightly acidic conditions (pH 5.0) at 37 °C. Compared to the *in vitro* release behavior of **β -CD-PLA-*b*-POEGMA** unimolecular micelles that encapsulated DOX via hydrophobic interaction,³¹ the cumulative release of DOX ($19 \pm 1.3\%$ at pH 7.2, and $49 \pm 0.6\%$ at pH 5.0) over 50 h from **CPOF-DOX** micelles was reduced under both conditions, which may be largely attributed to the improved stability of the Schiff-base linkage between DOX and **CPOF**. Compared to other micellar drug carriers, for instance, those formed by linear amphiphilic PEG-*b*-PLA block copolymers which released more than 80% drug in 24 h,⁵¹ the drug release kinetics of **CPOF-DOX** is significantly slower. Such enhanced sustainable release behavior, which is further reflected from the fluorescence imaging results (Figure 5) discussed later as well as other polymeric prodrug systems,^{12,13} is important to minimize any undesired drug leaching and side effects of toxicity towards healthy tissues.

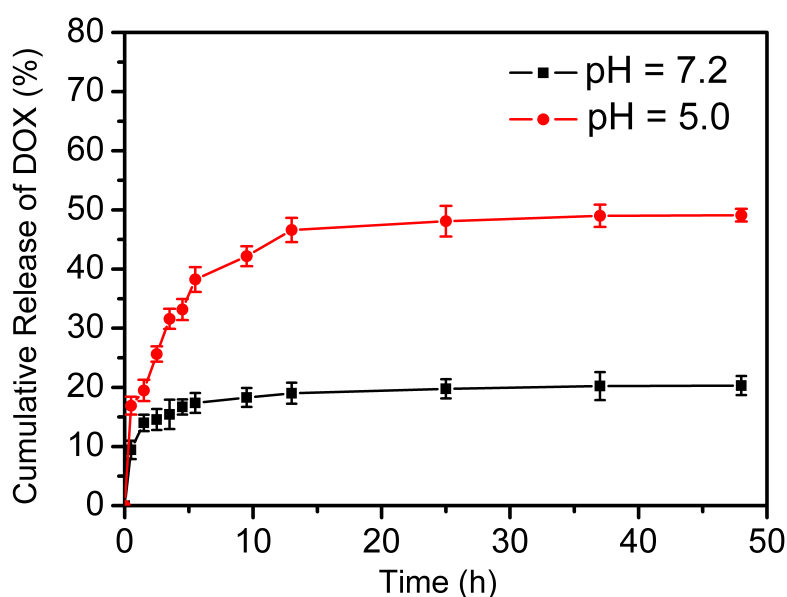


Figure 4. The *in vitro* drug release of CPOF-DOX micelles in PBS at pH 7.2 and pH 5.0 at 37 °C.

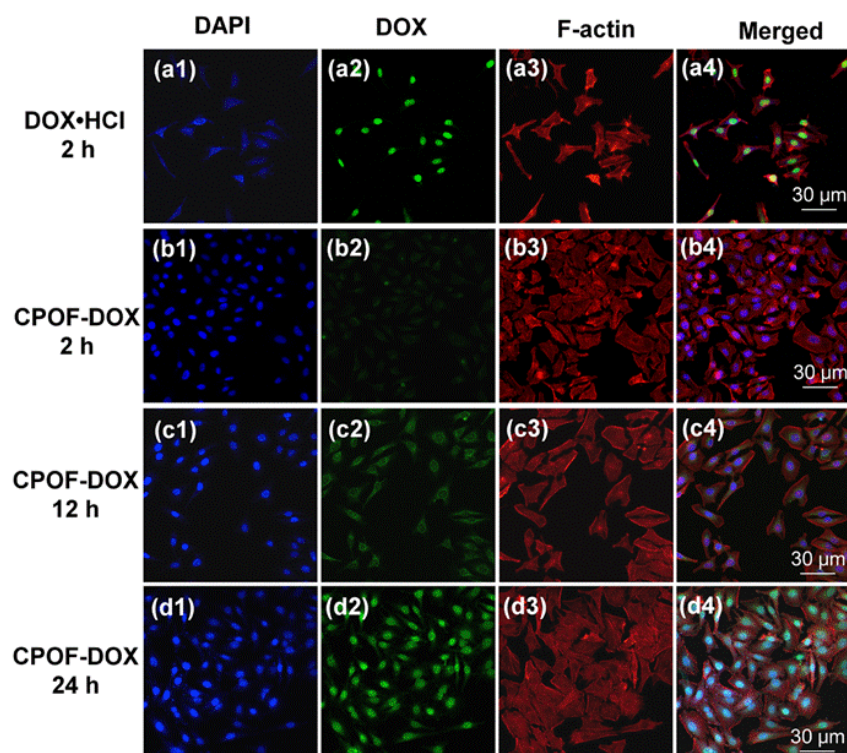


Figure 5. Drug internalization and localization in HeLa cells after incubation with carrier-free DOX•HCl (a 1-a 4) and CPOF-DOX (b-d) for 2 (b 1-b 4), 12 (c 1-c 4) and 24 h (d 1-d 4), respectively. The fluorescence of DAPI, DOX, and Alexa Fluor® 633 phalloidin (for labeling F-actin in the cell membrane) was pseudo-labeled with blue, green, and red, respectively.

We further investigated intracellular localization of the carrier-free DOX and **CPOF-DOX** unimolecular micelles in HeLa cell lines using confocal laser scanning microscopy (CLSM). Figure 5 shows three channels consisting of stained nuclei by DAPI, the fluorescence of DOX and the F-actin stained by Alexa Fluor 633 Phalloidin. After 2 h incubation with HeLa cells, the images (Figure 5a) show that all of carrier-free DOX accumulate in the nuclei that overlap with fluorescence of DAPI. In contrast, the fluorescence (FL) images (Figure 5b) of the same type of cells incubated with **CPOF-DOX** micelles over 2 h showed rather weak FL signal from **CPOF-DOX**.

It remained unclear whether such weak FL intensity was due to the insufficient uptake of **CPOF-DOX** micelles by the cells during such short incubation time, given the fact that the FL of DOX units was quenched due to their aggregation in **CPOF-DOX** unimolecular micelles (Figures S4 and S9). Even if the **CPOF-DOX** micelles were internalized by the cells, it might not be possible for the cells to induce significant dissociation of DOX from the micellar matrices within such short incubation time (2 h). When the time of cell incubation was increased to 12 h, obvious internalization of **CPOF-DOX** micelles by the cells was observed (Figure 5c) and most of DOX molecules accumulated around the nuclei, together with a small population released to the nuclei. Further increase of the incubation time to 24 h resulted in more release of the DOX from the **CPOF-DOX** micelles and significant accumulation in nuclei of HeLa cells (Figure 5d). These imaging results suggest that, at the beginning stage (< 12 h) of incubation with HeLa cells, most of DOX units remained associated with **CPOF** micelles and located mainly in the cytoplasm of the cells. With the incubation time elongated up to 24 h, the acidic intracellular environment of HeLa cells may promote the dissociation of the Schiff-base linkage in **CPOF-DOX** micelles and release of DOX small molecules which penetrate into the cell nuclei more easily than the micelles.

The step-wise intracellular release behavior of **CPOF-DOX** observed above is different from the exclusive and relatively fast nuclear-localization of DOX delivered by β -CD-poly(LA₂₄-*b*-OEGMA₁₂)/DOX micelles over 6 h incubation in the same type of cells,³¹ and are in consistent with the improved stability of Schiff-base linkage

between DOX and **CPOF** as well as the *in vitro* release results shown in Figure 5. Given the fact that DOX suppresses tumor proliferation by intercalating DNA,⁵² the controllable and sustainable delivery of DOX via **CPOF-DOX** unimolecular micelles into nuclei of HeLa cells suggests the promising applications in cancer treatment.

In Vitro Cytotoxicity.

Finally, we studied the cytotoxicities of the blank **CPOF** micelles and **CPOF-DOX** micelles vs. carrier-free DOX•HCl. Figure S10 (Supporting Information) shows that no obvious cytotoxicity was observed in HeLa cells which were incubated with the blank **CPOF** micelles with a concentration up to 400 $\mu\text{g mL}^{-1}$. In contrast, **CPOF-DOX** micelles showed some-extent toxicity to HeLa cells (Figure 6). For instance, the **CPOF-DOX** micelles containing 20 $\mu\text{g mL}^{-1}$ of DOX killed ca. 40% HeLa cells over 72 h. Moreover, the **CPOF-DOX** micelles showed lower cytotoxicity as compared with the carrier-free DOX•HCl with the same concentration range from 1.25 to 20 $\mu\text{g mL}^{-1}$. The relatively lower toxicity of **CPOF-DOX** micelles can be mainly attributed to slower releasing and accumulation of DOX due to chemical bonding with polymer, which is consistent with the results shown in the CLSM images (Figure 5).

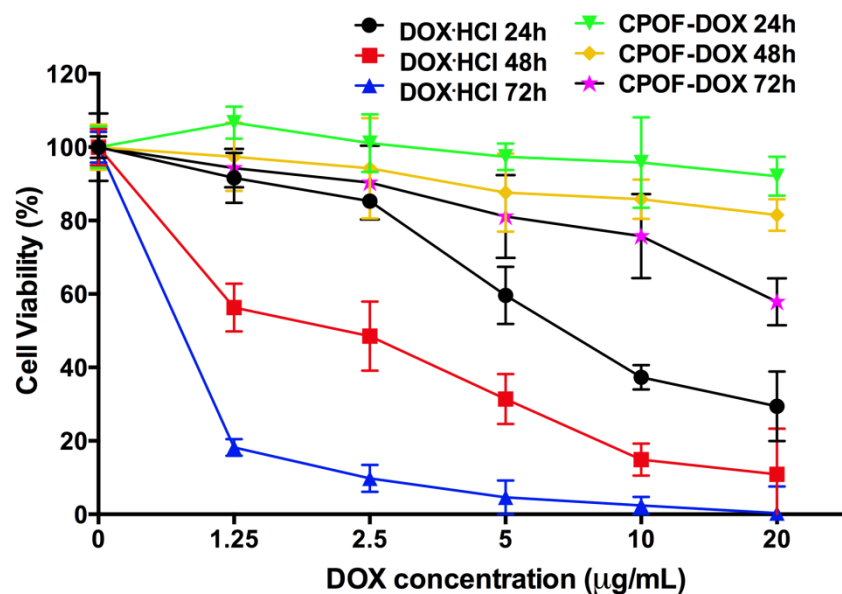


Figure 6. Cell viability of HeLa cells tested by PrestoBlue assay after treatment with different concentrations of carrier-free DOX·HCl and CPOF-DOX over 24, 48 and 72 h, respectively. Cells without treatment were used as control. Data were shown as means \pm SD (n = 5).

4. CONCLUSION

We have presented a new anticancer drug delivery system of unimolecular micelles formed by star-like amphiphilic copolymers with β -cyclodextrin as the core, from which statistical copolymers consisting of functionable benzo-aldehyde groups and hydrophilic poly[(oligo ethylene glycol) methyl ether methacrylate] were grafted from via ATRP. Anticancer drug DOX was covalently linked to the benzoaldehyde groups of the copolymers through pH-sensitive Schiff-base bonds. Each of the DOX-loaded star-like copolymer formed unimolecular micelles with an average diameter of 18 nm in aqueous media. Both the in vitro release data and the confocal fluorescence imaging results proved the enhanced stability of DOX covalently linked in **CPOF**

unimolecular micelles and the more controllable release kinetics compared to previous micellar drug carriers with noncovalently encapsulated DOX. The results suggest that the unimolecular micelles based on β -CD-core copolymers covalently linked with DOX via pH-responsive Schiff base linkage are a promising anticancer drug delivery system for future animal study and clinical trials for cancer treatment.

ASSOCIATED CONTENT

Supporting Information. The synthetic route to CPOF-DOX; the calibration curve of UV-vis absorbance at 495 nm of DOX in DMSO; the FTIR spectra of CPOF and CPOF-DOX; the DLS histograms of CPOF at different concentrations and in different solvents; the UV-vis spectra and digital photograph of CPOF, free DOX and CPOF-DOX, the DLS histograms of DOX at different concentrations in DMSO; the FL emission spectra of DOX and CPOF-DOX; the calibration curve of FL emission intensity at 550 nm of DOX in water; cell viability of HeLa cells after treatment with the polymer CPOF at various concentrations tested by PrestoBlue assay.

AUTHOR INFORMATION

Corresponding Authors

*(Mingfeng Wang) E-mail: mfwang@ntu.edu.sg

Notes

The authors declare no competing financial interest.

ACKNOWLEDGMENT

M.W. is grateful for the funding support through a start-up grant (M4080992.120) of

Nanyang Assistant Professorship from the Nanyang Technological University, and AcRF Tier 2 (ARC 36/13) from the Ministry of Education, Singapore. C. Y. and S.H. gratefully acknowledge the Ph.D. research scholarships from Nanyang Technological University.

REFERENCES

1. Duncan, R. Polymer conjugates as anticancer nanomedicines. *Nat. Rev. Cancer* **2006**, *6*, 688-701.
2. Zhang, S. Y.; Zou, J.; Elsabahy, M.; Karwa, A.; Li, A.; Moore, D. A.; Dorshow, R. B.; Wooley, K. L. Poly (ethylene oxide)-block-polyphosphester-based paclitaxel conjugates as a platform for ultra-high paclitaxel-loaded multifunctional nanoparticles. *Chem. Sci.* **2013**, *4*, 2122-2126.
3. Tong, R.; Cheng, J. J. Anticancer polymeric nanomedicines. *J. Macromol. Sci., Part C: Polym. Rev.* **2007**, *47*, 345-381.
4. Aljabali, A. A. A.; Shukla, S.; Lomonossoff, G. P.; Steinmetz, N. F.; Evans, D. J. Cpmv-Dox delivers. *Mol. Pharmacol.* **2012**, *10*, 3-10.
5. Gu, Y. D.; Zhong, Y. N.; Meng, F. H.; Cheng, R.; Deng, C.; Zhong, Z. Y. Acetal-linked paclitaxel prodrug micellar nanoparticles as a versatile and potent platform for cancer therapy. *Biomacromolecules* **2013**, *14*, 2772-2780.
6. Siegel, R.; DeSantis, C.; Virgo, K.; Stein, K.; Mariotto, A.; Smith, T.; Cooper, D.; Gansler, T.; Lerro, C.; Fedewa, S.; Lin, C.; Leach, C.; Cannady, R. S.; Cho, H.; Scoppa, S.; Hachey, M.; Kirch, R.; Jemal, A.; Ward, E. Cancer treatment and survivorship statistics, 2012. *CA-Cancer. J. Clin.* **2012**, *62*, 220-241.

7. Lee, S. M.; Nguyen, S. T. Smart nanoscale drug delivery platforms from stimuli-responsive polymers and liposomes. *Macromolecules*. **2013**, *46*, 9169-9180.
8. Rui, Y. J.; Wang, S. S.; Low, P. S.; Thompson, D. H. Dipalmitoylcholine-folate liposomes: an efficient vehicle for intracellular drug delivery. *J. Am. Chem. Soc.* **1998**, *120*, 11213-11218.
9. Al-Jamal, W. T.; Kostarelos, K. Liposomes: from a clinically established drug delivery system to a nanoparticle platform for theranostic nanomedicine. *Acc. Chem. Res.* **2011**, *44*, 1094-1104.
10. Harrisson, S.; Nicolas, J.; Maksimenko, A.; Bui, D. T.; Mougin, J.; Couvreur, P. Nanoparticles with in vivo anticancer activity from polymer prodrug amphiphiles prepared by living radical polymerization. *Angew. Chem. Int. Ed.* **2013**, *52*, 1678-1682.
11. Bui, D. T.; Maksimenko, A.; Desmaële, D.; Harrisson, S.; Vauthier, C.; Couvreur, P.; Nicolas, J. Polymer prodrug nanoparticles based on naturally occurring isoprenoid for anticancer therapy. *Biomacromolecules* **2013**, *14*, 2837-2847.
12. Ke, X. Y.; Coady, D. J.; Yang, C.; Engler, A. C.; Hedrick, J. L.; Yang, Y. Y. pH-sensitive polycarbonate micelles for enhanced intracellular release of anticancer drugs: a strategy to circumvent multidrug resistance. *Polym. Chem.* **2014**, *5*, 2621-2628.
13. Yu, Y.; Chen, C. K.; Law, W. C.; Sun, H. T.; Prasad, P. N.; Cheng, C. A. Degradable brush polymer-drug conjugate for pH-responsive release of doxorubicin. *Polym. Chem.* **2015**, *6*, 953-961.

14. Boas, U.; Heegaard, P. M. H. Dendrimers in drug research. *Chem. Soc. Rev.* **2004**, 33, 43-63.
15. Ma, X. P.; Zhou, Z. X.; Jin, E.; Sun, Q. H.; Zhang, B.; Tang, J. B.; Shen, Y. Q. Facile synthesis of polyester dendrimers as drug delivery carriers. *Macromolecules.* **2012**, 46, 37-42.
16. Chen, H. T.; Neerman, M. F.; Parrish, A. R.; Simanek, E. E. Cytotoxicity, hemolysis, and acute in vivo toxicity of dendrimers based on melamine, candidate vehicles for drug delivery. *J. Am. Chem. Soc.* **2004**, 126, 10044-10048.
17. Li, T. Y.; Smet, M.; Dehaen, W.; Xu, H. P. Selenium–platinum coordination dendrimers with controlled anti-cancer activity. *ACS Appl. Mater. Interfaces.* **2016**, 8, 3609-3614.
18. Liong, M.; Lu, J.; Kovichich, M.; Xia, T.; Ruehm, S. G.; Nel, A. E.; Tamanoi, F.; Zink, J. I. Multifunctional inorganic nanoparticles for imaging, targeting, and drug delivery. *ACS Nano.* **2008**, 2, 889-896.
19. Auffan, M.; Rose, J.; Bottero, J.-Y.; Lowry, G. V.; Jolivet, J.-P.; Wiesner, M. R. Towards a definition of inorganic nanoparticles from an environmental, health and safety perspective. *Nat. Nanotechnol.* **2009**, 4, 634-641.
20. Riedinger, A.; Leal, M. P.; Deka, S. R.; George, C.; Franchini, I. R.; Falqui, A.; Cingolani, R.; Pellegrino, T. “Nanohybrids” based on pH-responsive hydrogels and inorganic nanoparticles for drug delivery and sensor applications. *Nano Lett.* **2011**, 11, 3136-3141.
21. Yu, M. K.; Jeong, Y. Y.; Park, J.; Park, S.; Kim, J. W.; Min, J. J.; Kim, K.; Jon, S.

- Drug-loaded superparamagnetic iron oxide nanoparticles for combined cancer imaging and therapy in vivo. *Angew. Chem. Int. Ed.* **2008**, *47*, 5362-5365.
22. Lohse, S. E.; Murphy, C. J. Applications of colloidal inorganic nanoparticles: from medicine to energy. *J. Am. Chem. Soc.* **2012**, *134*, 15607-15620.
23. Slowing, I. I.; Trewyn, B. G.; Giri, S.; Lin, V. S. Y. Mesoporous silica nanoparticles for drug delivery and biosensing applications. *Adv. Funct. Mater.* **2007**, *17*, 1225-1236.
24. Lu, J.; Liong, M.; Zink, J. I.; Tamanoi, F. Mesoporous silica nanoparticles as a delivery system for hydrophobic anticancer drugs. *Small.* **2007**, *3*, 1341-1346.
25. Zeng, L. W.; Li, Y.; Li, T. Y.; Cao, W.; Yi, Y.; Geng, W. J.; Sun, Z. W.; Xu, H. P. Selenium–platinum coordination compounds as novel anticancer drugs: selectively killing cancer cells via a reactive oxygen species (ROS)-mediated apoptosis route. *Chem. Asian J.* **2014**, *9*, 2295-2302.
26. Xu, Z. G.; Liu, S. Y.; Kang, Y. J.; Wang, M. F. Glutathione- and pH-responsive nonporous silica prodrug nanoparticles for controlled release and cancer therapy. *Nanoscale.* **2015**, *7*, 5859-5868.
27. Bae, Y.; Fukushima, S.; Harada, A.; Kataoka, K. Design of environment-sensitive supramolecular assemblies for intracellular drug delivery: Polymeric micelles that are responsive to intracellular pH change. *Angew. Chem. Int. Ed.* **2003**, *115*, 4788-4791.
28. Nasongkla, N.; Bey, E.; Ren, J.; Ai, H.; Khemtong, C.; Guthi, J. S.; Chin, S. F.; Sherry, A. D.; Boothman, D. A.; Gao, J. M. Multifunctional polymeric micelles as cancer-targeted, MRI-ultrasensitive drug delivery systems. *Nano Lett.* **2006**, *6*,

2427-2430.

29. Stenzel, M. H. RAFT polymerization: an avenue to functional polymeric micelles for drug delivery. *Chem. Commun.* **2008**, 3486-3503.
30. Cabral, H.; Matsumoto, Y.; Mizuno, K.; Chen, Q.; Murakami, M.; Kimura, M.; Terada, Y.; Kano, M. R.; Miyazono, K.; Uesaka, M.; Nishiyama, N.; Kataoka, K. Accumulation of sub-100 nm polymeric micelles in poorly permeable tumours depends on size. *Nat. Nanotechnol.* **2011**, 6, 815-823.
31. Xu, Z. G.; Liu, S. Y.; Liu, H.; Yang, C. J.; Kang, Y. J.; Wang, M. F. Unimolecular micelles of amphiphilic cyclodextrin-core star-like block copolymers for anticancer drug delivery. *Chem. Commun.* **2015**, 51, 15768-15771.
32. Jones, M. C.; Ranger, M.; Leroux, J. C. pH-sensitive unimolecular polymeric micelles: synthesis of a novel drug carrier. *Bioconjugate Chem.* **2003**, 14, 774-781.
33. Ai, H.; Flask, C.; Weinberg, B.; Shuai, X. T.; Pagel, M. D.; Farrell, D.; Duerk, J.; Gao, J. Magnetite-loaded polymeric micelles as ultrasensitive magnetic-resonance probes. *Adv. Mater.* **2005**, 17, 1949-1952.
34. Kim, B. S.; Park, S. W.; Hammond, P. T. Hydrogen-bonding layer-by-layer-assembled biodegradable polymeric micelles as drug delivery vehicles from surfaces. *ACS Nano.* **2008**, 2, 386-392.
35. Cao, W.; Gu, Y. W.; Meineck, M.; Li, T. Y.; Xu, H. P. Tellurium-containing polymer micelles: competitive-ligand-regulated coordination responsive systems. *J. Am. Chem. Soc.* **2014**, 136, 5132-5137.
36. Xu, Z. G.; Liu, S. Y.; Kang, Y. J.; Wang, M. F. Glutathione-responsive polymeric

- micelles formed by a biodegradable amphiphilic triblock copolymer for anticancer drug delivery and controlled Release. *ACS Biomater. Sci. & Eng.* **2015**, *1*, 585-592.
37. Barenholz, Y. C. Doxil®—the first FDA-approved nano-drug: lessons learned. *J. Controlled Release* **2012**, *160*, 117-134.
38. Kim, T. Y.; Kim, D. W.; Chung, J. Y.; Shin, S. G.; Kim, S. C.; Heo, D. S.; Kim, N. K.; Bang, Y. J. Phase I and pharmacokinetic study of Genexol-PM, a cremophor-free, polymeric micelle-formulated paclitaxel, in patients with advanced malignancies. *Clin. Cancer Res.* **2004**, *10*, 3708-3716.
39. Oerlemans, C.; Bult, W.; Bos, M.; Storm, G.; Nijssen, J. F. W.; Hennink, W. E. Polymeric micelles in anticancer therapy: targeting, imaging and triggered release. *Pharm. Res.* **2010**, *27*, 2569-2589.
40. Webb, B. A.; Chimenti, M.; Jacobson, M. P.; Barber, D. L. Dysregulated pH: a perfect storm for cancer progression. *Nat. Rev. Cancer.* **2011**, *11*, 671-677.
41. Pang, X. C.; Zhao, L.; Han, W.; Xin, X. K.; Lin, Z. Q. A general and robust strategy for the synthesis of nearly monodisperse colloidal nanocrystals. *Nat. Nanotechnol.* **2013**, *8*, 426-431.
42. Ishii, T.; Otsuka, H.; Kataoka, K.; Nagasaki, Y. Preparation of functionally PEGylated gold nanoparticles with narrow distribution through autoreduction of auric cation by r-biotinyl-PEG-block-[poly(2-(N,N-dimethylamino)ethyl methacrylate)]. *Langmuir.* **2004**, *20*, 561-564.
43. Akiyama, Y.; Harada, A.; Nagasaki, Y.; Kataoka, K. Synthesis of poly(ethylene glycol)-block-poly(ethylenimine) possessing an acetal group at the PEG End.

Macromolecules. **2000**, *33*, 5841-5845.

44. Rossi, N. A. A.; Zou, Y. Q.; Scott, M. D.; Kizhakkedathu, J. N. RAFT synthesis of acrylic copolymers containing poly(ethyleneglycol) and dioxolane functional groups: toward well-defined aldehyde containing copolymers for bioconjugation.

Macromolecules. **2008**, *41*, 5272-5282.

45. Hwang, J.; Li, R. C.; Maynard, H. D. Well-defined polymers with activated ester and protected aldehyde side chains for bio-functionalization. *J. Controlled Release*.

2007, *122*, 279-286.

46. Nagasaki, Y.; Okada, T.; Scholz, C.; Iijima, M.; Kato, M.; Kataoka, K. The reactive polymeric micelle based on an aldehyde-ended poly(ethylene glycol)/poly(lactide) block copolymer. *Macromolecules*. **1998**, *31*, 1473-1479.

47. Cao, C. W.; Yang, K.; Wu, F.; Wei, X. Q.; Lu, L. C.; Cai, Y. L. Thermally induced swellability and acid-labile dynamic properties of microgels of copolymers based on PEGMA and aldehyde-Functionalized Monomer. *Macromolecules*. **2010**, *43*, 9511-9521.

48. Shi, M.; Li, A.-L.; Liang, H.; Lu, J. Reversible Addition–Fragmentation Transfer Polymerization of a novel monomer containing both aldehyde and ferrocene functional groups. *Macromolecules*. **2007**, *40*, 1891-1896.

49. Nguyen, T. K.; Selvanayagam, R.; Ho, K. K. K.; Chen, R. X.; Kutty, S. K.; Rice, S. A.; Kumar, N.; Barraud, N.; Duong, H. T. T.; Boyer, C. Co-delivery of nitric oxide and antibiotic using polymeric nanoparticles. *Chem. Sci*. **2016**, *7*, 1016-1027.

50. Sun, G. R.; Cheng, C.; Wooley, K. L. Reversible Addition Fragmentation Chain

Transfer Polymerization of 4-vinylbenzaldehyde. *Macromolecules*. **2007**, *40*, 793-795.

51. Shin, H. C.; Alani, A. W. G.; Rao, D. A.; Rockich, N. C.; Kwon, G. S. Multi-drug loaded polymeric micelles for simultaneous delivery of poorly soluble anticancer drugs. *J. Controlled Release*. **2009**, *140*, 294-300.

52. Xu, X.; Persson, H. L.; Richardson, D. R. Molecular pharmacology of the interaction of anthracyclines with iron. *Mol. Pharmacol*. **2005**, *68*, 261-271.

TOC figure

